Solid State Communications 164 (2013) 11–15

Contents lists available at SciVerse ScienceDirect

Solid State Communications

journal homepage: www.elsevier.com/locate/ssc

Localization length in the quasi one-dimensional disordered system revisited

Vladimir Gasparian [a,*], Emilio Cuevas [b]

[a] Department of Physics, California State University, Bakersfield, CA 93311, USA
[b] Departamento de Física, Universidad de Murcia, E-30071 Murcia, Spain

ARTICLE INFO

Article history:
Received 15 March 2012
Received in revised form
26 February 2013
Accepted 30 March 2013
by H. Akai
Available online 6 April 2013

Keywords:
A. Disordered systems
D. Quantum localization
D. Electronic transport

ABSTRACT

We have provided a complete description of the electron localization length (LL) in quasi-one dimensional (Q1D) disordered quantum wire with hard wall and periodic boundary conditions. Presented analytical expressions for LL are in excellent agreement with numerical calculations, exact up to order W^2 (W being the disorder strength), and valid for an arbitrary number of propagating and evanescent channels. We have calculated the average conductance in Q1D systems, establish relationship between various lengths and show that it basically differs from 1D case.

1. Introduction

A quasi-one dimensional (Q1D) geometry, as a model for a disordered wire, is of great interest in condensed matter theory. The electronic transport problem in weakly disordered Q1D systems can be solved analytically within some approximations (see, e.g., [1,2] for details). The Dorokhov–Mello–Pereyra–Kumar (DMPK) equation [3,4] and random matrix theory for the transfer matrix (see, e.g., Refs. [2,5]) are the two successful approaches which are generally applied to describe the behavior of conductance in a disordered wire. These two approaches give very similar solutions for the probability distribution of conductance in Q1D and can explain some universal properties of electron transmission. The DMPK theory predicts that the localization length (LL) is $\xi_M \approx [\beta(M-1)+2]l$, where M is the number of the propagating channels and l is the phenomenological mean free path, which measures the strength of the disorder. $\beta = 1, 2$ and 4 for the orthogonal, unitary and symplectic systems, respectively. However, the DMPK theory contains only one parameter, the mean free path l, which is viewed as a fixed parameter. Hence, the question how LL explicitly depends not only on energy E, but also on the coupling constants and the type of boundary conditions in Q1D disordered systems is left out in these analyses. What we are trying to point out is that in spite of the progress which has been made towards a characterization of the localization in Q1D systems, microscopic analytic studies of LL as a quantum parameter of fundamental importance have still not been achieved.

This long-standing problem has been approached from different points of view [6–8,11–13]. The first step in this direction was done by Dorokhov in Ref. [6], who calculated the LL of M random tight-binding (TB) chains with random site-energies. The LL in a weak disordered regime was obtained by the author for a Q1D wire with M channels and was found to be independent of the number of channels M. This result was questioned by Heinrichs [7], where it was shown that for weak disorder and for coupled two- and three-chain systems ($M = 2, 3$) the inverse LL is proportional to M, in contrast to the result of Ref. [6]. However, this approach, adopted in [7] and based on a scattering matrix treatment of conductance, does not allow the author to extend his studies of LL to Q1D systems with larger numbers of scattering channels M. Recently, progress has been made in taking into account an arbitrary number of channels in the calculation of LL. Römer and Schulz-Baldes [8], using a perturbative formula for the lowest Lyapunov exponent (the inverse LL) for the Q1D TB Anderson strip model, obtained LL's dependence on energy E, propagating modes M (M is even) and disorder strength W (see Eq. (7) of [8]). This rigorous perturbative formula for the smallest Lyapunov exponent is valid for a *numerical study only* and for a *periodic boundary* (PB) conditions. To get an approximate analytical expression for LL, see Eq. (13), the authors of Ref. [8] in Eq. (7) replaced so-called Birkhoff averages by M^{-2} (for more details see [8]). Note also that the weak disorder expansion of the Lyapunov exponents of a product of random matrices and the sum of the first p Lyapunov exponents were calculated in some specific cases in Refs. [9,10]. A non-perturbative analytical approach, based on Green's function formalism to solve the Dyson equation exactly in

* Corresponding author. Tel.: +1 661 654 6004; fax: +1 661 654 2693.
E-mail addresses: vgasparyan@csub.edu (V. Gasparian), ecr@um.es (E. Cuevas).
URL: http://bohr.fcu.um.es/miembros/ecr/ (E. Cuevas).

0038-1098/$ - see front matter © 2013 Elsevier Ltd. All rights reserved.
http://dx.doi.org/10.1016/j.ssc.2013.03.029

Q1D and two-dimensional (2D) disordered systems without any restriction on the numbers of impurities and modes, was developed in Refs. [11–13]. For a tight-binding (TB) Hamiltonian with several modes and on-site disorder the electron's scattering matrix elements T_{nm} were analytically calculated exactly for an arbitrary impurity profile without using any perturbative theory and without actually determining the eigenfunctions. Later on in the weak disordered regime the wire conductance $G=\sum_{nm}T_{nm}T^{*}_{nm}$ (in units of e^2/h) was calculated [11–13]. In these papers only hard wall (HW) conditions were discussed, which correspond to arranging the parallel equidistant chains on a plane.

The main objective of our paper is, based on the careful numerical analysis, to derive the explicit expressions for LL in a Q1D system with HW and PB conditions for an arbitrary number of channels M (even and odd), and to verify that they are in excellent agreement with numerical data. In our numerical simulations we used Kubo's formula for computing conductivity. This formalism is quite reliable because it is based on direct calculations of the conductance and provides trustworthy results, no matter how small the range of the considered quantity is (see [14,15] for details). The numerical results were compared with the existing analytical expressions of LL, calculated in Refs. [6–8,11–13]. Surprisingly, our numerical calculations show that none of these expressions for LL can be obtained numerically. Particularly, LLs calculated in Refs. [6,7,11,12] result in an incorrect dependence on M, because of their definition of the inverse localization length was missing a M^{-1} normalization factor. LLs calculated in Refs. [8,13] correctly predicted the M dependence, but failed to provide the exact magnitude of LL.

The origin of the disagreement between the present numerical data and the theoretical results of Refs. [8,13], as we will see later on, is due to two main factors: (i) Since it is not easy to calculate the right-hand term of Eq. (7), theoretical calculations assume that in the weak disordered regime the length $\langle \ln G\rangle$ can be replaced by length $\ln\langle G\rangle$ (or $\ln\langle 1/G\rangle$) and by expanding to the lowest order of the powers of the disorder and, after averaging over realizations, one can get a closed analytical expression for LL in the Q1D system ($\langle\cdots\rangle$ denotes averaging over disorder realizations). However, because of not self-averaging the conductance G, these lengths do not agree with each other and thus lead to a different answer for LL. Note that the same type of problem exists also in 1D disordered systems where, in the weak disordered limit, LLs, obtained numerically and analytically, differ by a factor of 2 (see e.g., [16–19]). (ii) As follows from the numerical analysis of the relationship between the different LLs in Q1D systems (see Eq. (4)), the right hand-side term is not zero. This is an essential piece of information, which allows us later on to justify the disagreement between the results of numerical simulations and theory and introduce new LLs for different boundary conditions in the transverse direction, which fit the numerical data very well.

It is worth noting that while in 1D the relationships between the various lengths are well known (e.g., $\langle \ln G\rangle = 4\ln\langle G\rangle = -\frac{1}{2}\ln\langle 1/G\rangle$ or $2\langle \ln\rho\rangle = \ln\langle\rho\rangle$, where ρ is the Landauer resistance), in Q1D, to the best of our knowledge, no such calculations have been previously reported. Our first goal consists in checking numerically what relationship exists for different lengths in the Q1D case. Once this is established, motivated by our doubts about the correctness of LLs results of Refs. [6–8,11–13] and to overcome the difficulty of the discrepancy, we have reconsidered the calculation of LL for the Q1D TB anisotropic Anderson model, using Green's function approach, developed in Refs. [11–13]. This is our second and main goal. The analytical results for LL with HW and PB conditions, Eqs. (9) and (11), are then compared with numerical results. Excellent agreement with analytical calculations can be achieved if one multiplies the expressions (9) and (11) by a factor 2 (as in pure 1D case) and shifts them up by ξ_1 for HW and by $\xi_1/2$ for PB conditions, respectively. $\xi_1 = 96\sin^2 k_1/W^2$ is the LL in a 1D disordered system, calculated in the weak disordered regime [20]. The shift, as it was mentioned, reflects the fact that the right-hand side of Eq. (4) is different from zero.

2. Q1D TB anisotropic Anderson model

Let us discuss a Q1D disordered lattice of size $L\times M$ described by the standard TB anisotropic Hamiltonian with nearest-neighbor transfers, t_x and t_y along the x- and y-directions, respectively

$$\mathcal{H}=\sum_{j=1}^{L}\sum_{l=1}^{M}|j,l\rangle\epsilon_{j,l}\langle j,l| - \sum_{j,l}\sum_{\delta=\pm 1}\{|j,l\rangle t_x\langle j+\delta,l| + |j,l\rangle t_y\langle j,l+\delta|\}, \quad (1)$$

where $|j,l\rangle$ is the atomic orbital at site (j,l) and $\epsilon_{j,l}$ is the strength of the random potential at site (j,l), assuming it to be uniformly distributed in the interval $(-W/2, W/2)$. The disordered region is connected to perfect leads on both ends, extended to $\pm\infty$ in the x-direction. L is the length of the system and M is the number of modes in the left and right leads. For simplicity we choose the lattice constant to be equal to 1. For further calculations we assume the existence of a confining potential $V_c(y)$ in the direction y. This potential leads to a set of transverse modes, whose actual values depend, however, on boundary conditions. For HW and PB conditions, the energy of the electron is given by the following dispersion relations:

$$E=\begin{cases} 2t_x\cos k_n + 2t_y\cos\dfrac{\pi n}{M+1}, & n=1,2,\ldots,M,\ \text{HW},\\ 2t_x\cos k_n + 2t_y\cos\dfrac{2\pi n}{M}, & n=0,1,\ldots,M-1,\ \text{PB}. \end{cases} \quad (2)$$

The appropriate eigenfunctions, $\psi_n(y_l)$, of the 1D Schrödinger equation with periodic potential of the chain of atoms along the y-direction with HW and PB conditions are ($l=1,2,\ldots,M$)

$$\psi_n(y_l)=\begin{cases} \sqrt{\dfrac{2}{M}}\sin\dfrac{\pi ln}{M+1}\ \text{HW},\\ \sqrt{\dfrac{2-\delta_{n,0}-\delta_{n,M/2}}{M}}\exp\left[i\dfrac{2\pi nl}{M}\right]\ \text{PB}. \end{cases} \quad (3)$$

3. Relationship between different lengths in Q1D systems

First we study the relationship between $\langle \ln G\rangle$ and $\ln\langle G\rangle$ in Q1D disordered systems, described by Eq. (1). Our numerical calculations show that these two lengths are connected through the relation

$$\langle \ln G\rangle - 4\ln\langle G\rangle = C. \quad (4)$$

The constant C is different for HW and PB conditions and for each case is determined numerically. C tends to zero in the 1D case as expected. The length L dependence of $\langle \ln G\rangle$ and $4\ln\langle G\rangle$ is plotted in Fig. 1 for $M=10$ and $W=1$. The slopes of the two lines are the same within error bars. For each value of W we used L' s that ensure that we are well inside the exponential decay (see Fig. 1).

For completeness, we show in the upper panel of Fig. 2 the $1/M$ dependence of the constant C for fixed disorder and energy for relatively large M. One can see that for $M\gg 1$ C decreases linearly, according to the asymptotic behavior of localization lengths (see [20] and Eq. (4)). Numerical data for the constant C versus energy are presented in the lower panel of Fig. 2. As expected, C is very sensitive to any change of the energy, as well as to the change of the boundary conditions (in Fig. 2 we have presented only the results for HW boundary conditions). Some technical details follow: to obtain the mean values $\langle\cdots\rangle$ we have used 10^5 independent realizations of the disordered strip. Assuming a Gaussian form

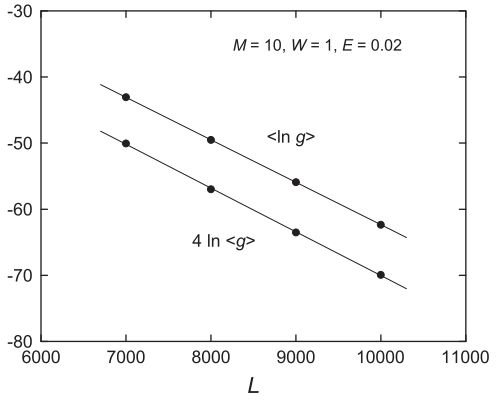

Fig. 1. Averaged logarithm of the conductance $\langle \ln G\rangle$ and logarithm of the average conductance $\ln\langle G\rangle$ as a function of the length L of the strip. The value of $C\approx 7.5$ and errors are smaller than the symbol's size.

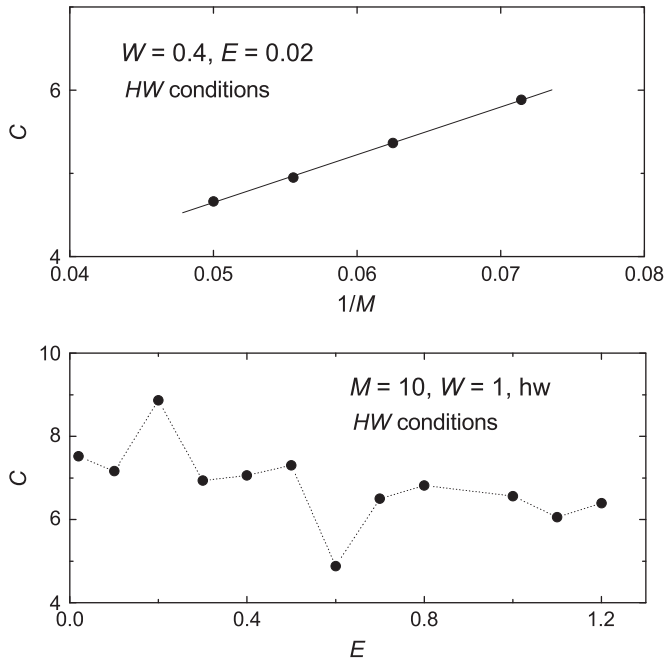

Fig. 2. The number of channels M and energy E dependence of the constant C in the case of HW condition.

(as we have checked) for the logarithm of the conductance, $z\equiv\ln G$, it is straightforward to show that the average of G is $\langle G\rangle = \int_0^M GP(G)\,dG = \int_0^M P(\ln G)\,dG$. Solving the last integral and combining it with the numerical results for $\langle \ln G\rangle$ and its variance σ^2 we get

$$\langle G\rangle = \frac{1}{2}\,\exp(\langle \ln G\rangle + \sigma^2/2)\,\mathrm{Erfc}\left[\frac{\langle \ln G\rangle + \sigma^2 - \ln M}{\sqrt{2}\sigma}\right], \tag{5}$$

where Erfc is the complementary error function.

4. Localization length in Q1D systems

4.1. All channels are propagating

Next, closely following Refs. [11–13], we evaluate the scattering matrix elements T_{nm}, in the weak disordered regime. This means that it is sufficient to restrict the expansion of the expressions of T_{nm} to first order in the $\epsilon_{j,l}$—the strength of the potential at site (j,l). In other words, in the evaluation we only kept the terms that are proportional to the electron's transmission amplitude from the isolated potential $\epsilon_{j,l}$. The result for the electron transmission amplitude T_{nm} is

$$T_{nm}\approx e^{ik_m(L-1)}\times\begin{cases}1-i\dfrac{\sum_{l=1}^{M}\sum_{j=1}^{L}\epsilon_{j,l}\psi_m(y_l)\psi_m^*(y_l)}{4DL_t\sin k_m} & \text{if } n=m,\\ -i\dfrac{\sum_{l=1}^{M}\sum_{j=1}^{L}\epsilon_{j,l}e^{i\phi_j}\psi_n(y_l)\psi_m^*(y_l)}{2L_t\sqrt{\sin k_n\sin k_m}} & \text{if } n\neq m,\end{cases} \tag{6}$$

where $A_l=(1/2L_t)\sum_{n=1}^{M}\psi_m(y_l)\psi_m^*(y_l)/\sin k_n$, $\phi_j=(k_n-k_m)(j-1)$ and $D=1+i\sum_{l=1}^{M}\sum_{j=1}^{L}\epsilon_{j,l}A_l$. The wave numbers k_n for the propagating modes are defined by Eq. (2), for HW and PB conditions, respectively. Similarly, L_t is equal to $M+1$ or M depending on the boundary conditions.

The inverse normalized LL ξ_M as a function of the system size L and modes M can be written as

$$\frac{1}{\xi_M} = -\lim_{L\to\infty}\frac{1}{2ML}\left\langle \ln\sum_{n,m}^{M}|T_{nm}^{(N)}|^2\right\rangle. \tag{7}$$

Now, replacing $\langle \ln G\rangle$ by $\ln\langle G\rangle$ and assuming that for weak disorder the transmission coefficients are close to 1 and thus the reflection coefficients are close to zero, we can expand the right-hand side of Eq. (7). Next, after ensemble averaging over the random potentials $\epsilon_{j,l}$ distributed uniformly according to the explicit expressions for T_{nm} of Eq. (6) and keeping the terms to order W^2, we arrive at the following expression for the inverse LL:

$$\frac{1}{\xi_M} = \frac{W^2}{96M^2}\sum_{l=1}^{M}\left[\sum_{n=1}^{M}\frac{\psi_n(y_l)\psi_n^*(y_l)}{\sin k_n}\right]^2 + \mathcal{O}(W^4), \tag{8}$$

which is valid for both boundary conditions.

4.1.1. Hard wall conditions

Using the explicit expressions for $\psi_n(y_l)$ (see Eqs. (3) and (8)) for the LL ξ_M with HW conditions, when the M channels are propagating, we obtain

$$\frac{1}{\xi_M^{HW}} = \frac{W^2}{192M^2(M+1)}\times\left[\sum_{n=1}^{M}\frac{3+\delta_{2n,M+1}}{\sin^2 k_n} + 2\sum_{n<p}^{M}\frac{2+\delta_{n+p,M+1}}{\sin k_n\sin k_p}\right]. \tag{9}$$

k_n is the Fermi wave vector of the n-th subband (channel) and is determined by the energy dispersion relation (2).

For $M=1$ it reduces to the LL ξ_1 for a 1D chain. If there is no coupling to the second, third, etc., modes, all k_n are equal, and after the summation over the modes, we find from Eq. (9) $\xi_M^{HW}=M\xi_1$. This result is somewhat expected: it confirms the prediction of Thouless [20] that in the limit of weak coupling ξ_M^{HW} must be proportional to M. Although one can get two correct limiting values ξ_1 and $\xi_{M\gg 1}$ from expression ξ_M^{HW}, Eq. (9), it fails to give the exact value of LL for an arbitrary M. A similar formula for a periodically arranged 2D δ-potential scatterers on a strip can be found in [13].

Our direct numerical computation of the LL for the Anderson model (1) shows that we can get an almost perfect agreement with the theoretical ξ_M^{HW}, Eq. (9) for $M\geq 2$, if we multiply the latter by a factor 2 and shift it up by ξ_1, i.e., redefine new LL χ_M^{HW}

$$\chi_M^{HW} = \frac{\xi_M^{HW}}{2}+\xi_1, \quad M\geq 2. \tag{10}$$

Fig. 3 shows the M mode dependence of χ_M^{HW}. The solid lines have been computed from Eq. (10) and the dots denote the result of numerical calculations. The good agreement found fully supports the validity of the analytical expression for χ_M^{HW}. The comparison is free of any adjustable parameter. We have checked that the analytical expression, Eq. (10), agrees very well with the numerical data in the whole range of vertical hopping parameter $0<t_y<1$ where the χ_M^{HW} is a linear function with respect to M. Note that for $0<t_y<1$ and energy $E=0.02$ all the modes are propagating, hence the expression is valid. The non-linearity starts when $t_y\geq 1$ and for

those t_y the numerical and analytical results start behaving differently due to the fact that the validity of formula (10) breaks down, i.e., in the spectrum began to appear evanescent modes (see Section 3.2).

4.1.2. Periodic boundary conditions

The result for the LL reads as

$$\frac{1}{\xi_M^{PB}} = \frac{W^2}{96}\begin{cases} \dfrac{1}{M^3}\left[\displaystyle\sum_{l=0}^{M/2}\frac{2-\delta_{l,0}-\delta_{l,M/2}}{\sin k_l}\right]^2 & \text{if } M \text{ even} \\ \dfrac{1}{(M-1)^3}\left[\displaystyle\sum_{l=0}^{(M-1)/2}\frac{2-\delta_{l,0}}{\sin k_l}\right]^2 & \text{if } M \text{ odd,} \end{cases} \tag{11}$$

where k_l must be defined from the dispersion relation (2). Like expression (9) Eq. (11) is valid only for propagating modes.

The process of deriving the expression for even M is quite straightforward. Using the explicit form of the electron wave function $\psi_n(y_l)$, (3) and Eq. (8) yields the desired result. The case for odd M requires special consideration. First, for the infinitely long periodic system ($W=0$) the conductance G is an *asymmetric* function of energy, which is in contrast to the *symmetric* behavior of G with even M modes. Second, the analysis of the conductance of the ideal TB model as a function of the energy (at fixed odd M) shows that the change from one plateau value to the next one is 2 (in units of e^2/h), while in the case of even M, it is 1. Formally this means that M must be replaced by $(M-1)$ in the expression of LL with even number of M. This conjecture was numerically tested and supported by the direct numerical calculation of the LL (see Fig. 4). It is clear that the difference between M and $(M-1)$ is negligible for large M, but may not be negligible for small M.

As in the case of HW condition we get an excellent agreement with the theoretical ξ_M^{PB}, Eq. (11) for $M\geq 2$, if we multiply the latter by a factor 2 and shift it up by $\xi_1/2$. The new LL χ_M^{PB} is

$$\chi_M^{PB} = \frac{\xi_M^{PB}}{2} + \frac{\xi_1}{2}, \quad M\geq 2. \tag{12}$$

In Fig. 4 we have tested the prediction of the analytical theory against the numerical results where the M mode dependence of χ_M^{PB}, Eq. (12) is shown. Solid lines have been computed from Eq. (12) and dots denote the result of numerical calculations. The good agreement between simulations (dots) with Eq. (12) is evident for a relatively large range of disorder W. In the right panel of Fig. 4 our numerical data for LL was compared with similar expression ξ (dashed line, M is even) from Ref. [8]

$$\frac{1}{\xi} \approx \frac{W^2}{96M^3}\sum_{l,m=0}^{M-1}\frac{2-\delta_{l,m}}{\sin k_l \sin k_m}. \tag{13}$$

One can see that the slope of the dashed line agrees with numerical calculations, but certainly there is a problem with an intercept and hence with accurate numerical values of LL. To get a correct value for LL, Eq. (13), for an arbitrary even M one needs the dashed line to shift up by about $0.39\xi_1$.

Note that for the energy $E=0.02$ and for the disorder range $0.4\leq W\leq 1$ the localization lengths do not show anomalous fluctuations near the band center [21].

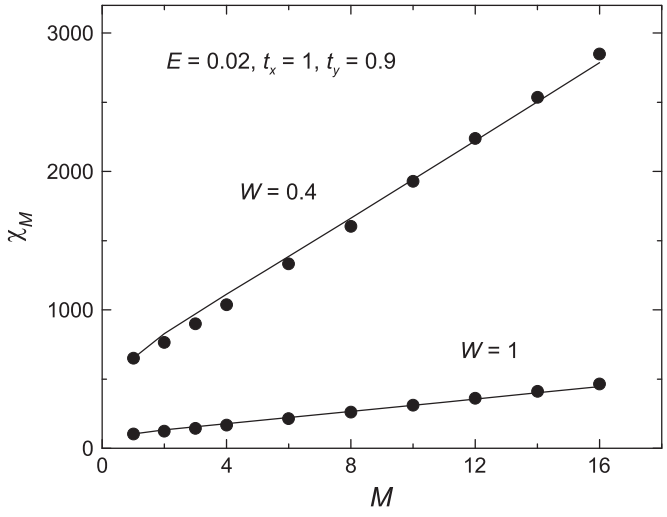

Fig. 3. The dependence of the localization length χ_M^{HW} on the number of modes M for disorder W=0.4 and 1.0. Dots are the numerical results and each data point corresponds to an average over 10^5 realizations of disorder (errors are smaller than the symbol's size). The solid lines represent the theoretical prediction, Eq. (10). At $E=0.02$ all modes are propagating.

4.2. M–ν evanescent channels

Our objective in this subsection is to extend our previous calculations of LL (see Eqs. (9) and (11)) in the case when only the first ν modes can propagate along the Q1D system, whereas $(M-\nu)$ cannot (M is the total number of channels). Hence we consider the case of $E_1 < E_2 < \cdots < E_\nu$. Proceeding along the same line as in Section 4, one can show that only minor modifications of the final expression for the LL, Eqs. (9) and (11), are required in order to include (M−ν) evanescent modes. In other words in the mentioned equations one should replace M^2 by ν^2 and the sum

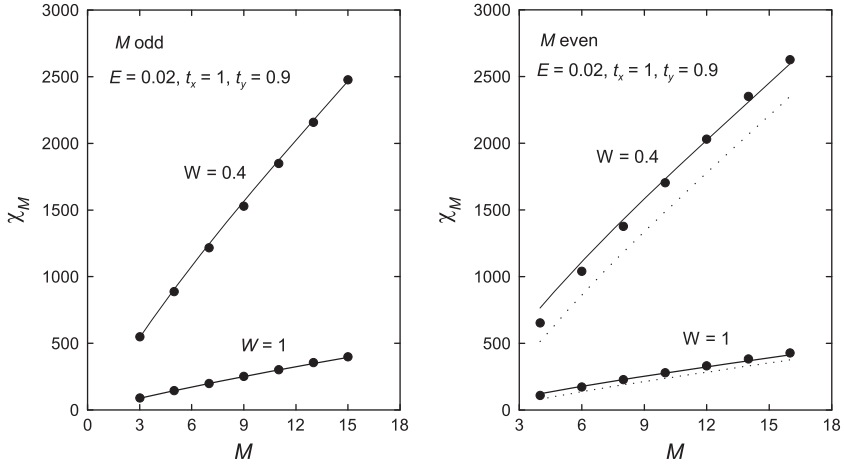

Fig. 4. M dependence of the localization length defined by Eq. (12). Dots are the numerical results. Left: M is odd. Right: M is even. Dashed line represents Eq. (13) (see [8]).

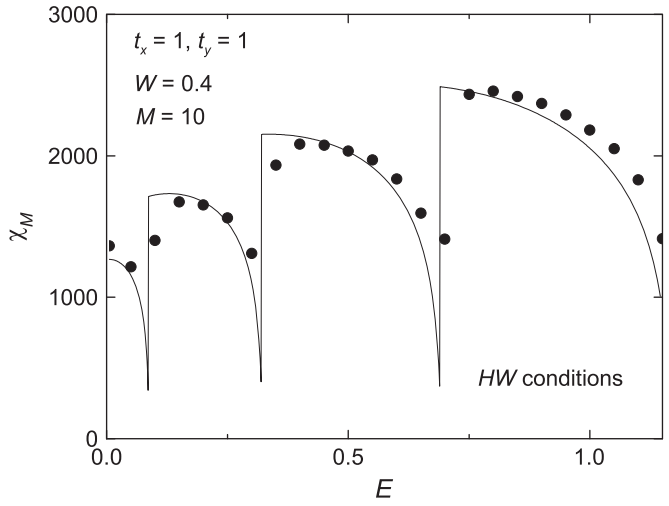

Fig. 5. The energy E dependence of the localization length χ_ν^{HW} in the case of HW condition (Eq. (14)). The parameters are disorder $W=0.4$, number of channels $M=10$ and horizontal and vertical hopping parameters t_x and t_y are equal to 1. Dots are the numerical results and the solid line represents the theoretical prediction, (14). At $E\geq 1.6$ in the spectrum we have 4 and more evanescent modes.

runs only up to ν propagating modes (in the case of odd M in the Eq. (11) $(M-1)^2$ must be replaced by $(\nu-1)^2$). For example, the expression for LL in the case of HW condition now reads as

$$\chi_\nu^{HW}=\frac{\xi_\nu^{HW}}{2}+\xi_1,\quad \nu\geq 2. \tag{14}$$

where ξ_ν^{HW} is analogous to Eq. (9) with appropriate changes

$$\frac{1}{\xi_\nu^{HW}}=\frac{W^2}{192\nu^2(M+1)}\times\left[\sum_{n=1}^{\nu}\frac{3+\delta_{2n,\nu+1}}{\sin^2 k_n}+2\sum_{n<p}^{\nu}\frac{2+\delta_{n+p,\nu+1}}{\sin k_n\,\sin k_p}\right]. \tag{15}$$

The reason for this restriction in such a simple way was pointed out in Refs. [22,12], in the analysis of role of evanescent states on the ensemble average conductance in multi-channels TB and 2D $\delta-$potential disordered systems for weak disorder. The main idea is that the use of the weak disorder approximation leads to the suppression of the effect of $(M-\nu)$ evanescent modes. Moreover, the presence of evanescent modes enhances the LL with respect to LL, for all the values of the Fermi energy, when evanescent modes are absent [12,22]. The reason is quite clear from a physical point of view: with increasing numbers of evanescent modes, the point-type scatterer becomes more and more transparent. As the number of evanescent modes increases towards infinity, we get perfect transmission which leads to perfect conductance and hence to the increase in LL [12,22–26]. This is confirmed in Fig. 5 where we show the energy E dependence of LL, given by Eq. (14), for fix disorder $W=0.4$ and number of channels $M=10$.

One can see that χ_ν^{HW} is decreasing monotonically with increasing E up to $E\approx 0.08$ (all modes are propagating, i.e. $\nu=M$). Then LL showing oscillatory behavior when E, starting from the value of $E\approx 0.08$, approaches the points $E_1=0.081$ (1 evanescent mode in spectrum), $E_2=0.317$ (2 evanescent modes in spectrum), $E_3=0.69$ (3 evanescent modes in spectrum), etc. The regions with jump discontinuity lie precisely on $E_{11-n}=2(1+\cos\pi n/11)$ values, when new evanescent mode appears in the spectrum. Note that an analogous oscillatory behavior shows also LL as a function of vertical hopping parameter t_y for fix disorder W, the number of channels M and horizontal hopping parameter t_x.

5. Summary

We have provided a complete description of LL in Q1D disordered quantum wire with hard wall and periodic boundary conditions for the case where propagating as well as evanescent channels are present. We pointed out that the relationship between various lengths in Q1D disordered systems obeys Eq. (4), which basically differs from 1D case because of a finite value of the right-hand side term C. Based on this new relationship, Eq. (4), we have presented the analytical expressions (10), (12) and (14) for LL which are in excellent agreement with numerical calculations, exact up to order W^2 (W being the disorder strength), and valid for an arbitrary number of propagating and evanescent channels. We show that the presence of evanescent modes enhances the LL with respect to the value obtained when evanescent modes are absent.

Acknowledgments

We thank T. Meyer for critical reading of the paper. The work was supported by FEDER and the Spanish DGI under Project no. FIS2010-16430.

References

[1] P. Markos, Acta Phys. Slovaca 56 (2006) 561.
[2] A. Mirlin, Phys. Rep. 326 (2000) 259.
[3] O.N. Dorokhov, JETP Lett. 36 (1982) 318.
[4] P.A. Mello, P. Pereyra, N. Kumar, Ann. Phys. (NY) 181 (1988) 290.
[5] C. Beenakker, Rev. Mod. Phys. 69 (1997) 731.
[6] O.N. Dorokhov, Phys. Rev. B 37 (1988) 10526.
[7] J. Heinrichs, J. Phys. Condens. Matter 15 (2003) 5025.
[8] R.A. Römer, H. Schulz-Baldes, Europhys. Lett. 68 (2004) 247.
[9] B. Derrida, E. Gardner, J. Phys. France 45 (1984) 1283.
[10] N. Zanon, B. Derrida, J. Stat. Phys. 50 (1988) 509.
[11] V. Gasparian, Phys. Rev. B 77 (2008) 113105.
[12] V. Gasparian, A. Suzuki, J. Phys. Condens. Matter 21 (2009) 405302.
[13] V. Gasparian, M. Cahay, E. Jódar, J. Phys. Condens. Matter 23 (2011) 045301.
[14] S. Datta, Electronic Transport in Mesoscopic Systems, Cambridge University Press, Cambridge, 1995.
[15] J.A. Vergés, E. Cuevas, M. Ortuño, E. Louis, Phys. Rev. B 58 (1998) R10143.
[16] B.S. Andereck, E. Abrahams, J. Phys. C: Solid State Phys. 13 (1980) L383.
[17] A. MacKinnon, B. Kramer, Rep. Prog. Phys. 56 (1993) 14689.
[18] V.M. Gasparian, B.L. Altshuler, A.G. Aronov, Z.H. Kasamaian, Phys. Lett. A 132 (1988) 201.
[19] V. Gasparian, A. Khachatrian, Solid State Commun. 85 (1993) 1061.
[20] D.J. Thouless, Phys. Rev. Lett. 39 (1977) 1167.
[21] M. Kappus, F. Wegner, Z. Phys. B—Condens. Matter 45 (1981) 15.
[22] J. Heinrichs, Phys. Rev. B 68 (2003) 155403.
[23] M. Cahay, M. Mclennan, S. Datta, Phys. Rev. B 37 (1988) 10125.
[24] P.F. Bagwell, J. Phys.: Condens. Matter 2 (1990) 6179.
[25] P.S. Deo, Phys. Rev. B 75 (2007) 235330.
[26] V. Vargimaidis, M. Polatoghlu, Phys. Rev. B 67 (2003) 245303.